Shock Tube Studies of the Acetylene and Ethylene Pyrolysis by UV Absorption

Tohru KOIKE* and Kihei MORINAGA

Department of Chemistry, National Defense Academy, Hashirimizu, Yokosuka 239

(Received July 22, 1980)

Absorption measurements at 216 and 230 nm of shock heated C_2H_2, $C_2H_2+H_2$, and C_2H_4 diluted in Ar were made over the temperature range 1800 K to 2600 K at half of atmospheric pressure. Absorptivities were evaluated for C_4H_2, which is the main product of C_2H_2 pyrolysis, as well as for C_2H_2 and C_2H_4. The relative value of C_4H_2 absorption was confirmed to decrease with the presence of H_2 in accordance with a computer modeling result using a 25-reaction mechanism. The time profile of C_4H_2 absorption could be modeled well with $k=10^{12.4}$ cm^3 mol^{-1} s^{-1} for the reaction $H_2+C_2H=C_2H_2+H$.

The pyrolysis of C_2H_2 in shock waves has been studied by many workers and has become explainable through computer modeling with a rather definite reaction mechanism.

Recently, two groups studied the C_2H_2 pyrolysis using real-time kinetic absorption spectroscopy and the laser schlieren method. Frank and Just[1] measured the [H] profile in the C_2H_2 pyrolysis by atomic resonance absorption spectroscopy (ARAS) in mixtures of C_2H_2 highly diluted in Ar to ppm order and evaluated the initiation reaction rate constant in the low pressure region. Tanzawa and Gardiner[2] did laser schlieren experiments on the C_2H_2 pyrolysis. They proposed a reaction mechanism, in which the experimental results obtained by TOF mass spectroscopy[3,4] and single pulse shock tube[5] as well as their laser schlieren results were analyzed by computer modeling studies. Their later efforts[6] led them to a final mechanism which accords with almost all of the experimental results from 625 to 3400 K.

The new mechanism of the C_2H_2 pyrolysis so derived is expected to improve the C_2H_4 pyrolysis mechanism, because C_2H_4 decomposes to C_2H_2 and H_2 by a molecular reaction very rapidly in the high temperature region.[7]

Cundall *et al.*[8] studied the C_2H_2 and C_2H_4 pyrolysis in shock waves by absorption spectroscopies with Xe-lamp and He–Ne laser. The reaction mechanism used by them was rather primitive and the values of heat of formation for C_2H and polyacetylene radicals are subject to correction,[1,2,9] though they could obtain qualitative information about soot formation.

The present paper is concerned with the C_2H_2 and C_2H_4 pyrolysis behind incident shock waves. The reaction features were examined by UV absorption at 216 and 230 nm and were interpreted more quantitatively by the computer modeling with a refined mechanism.[6]

Experimental

The shock tube used in this study has been described in detail already.[10]

The light from a D_2-lamp (Hamamatsu-TV, L544) or Xe-lamp (Ushio, UXL500D), made parallel with a quartz lens, was measured using a photomultiplier (Hamamatsu-TV, R208) with a monochrometer (Jarrell-Ash, JE25) after passing through two shock tube windows. The output from the photomultiplier was displayed on an oscilloscope (Tektronix, 7603).

The signal from piezo-gauges mounted on the shock tube every 10 cm was detected by a universal counter (Takeda-Riken, TR5002). Shock temperature was calculated from the measured shock velocity assuming full relaxation and no chemical reaction.

Gases used were 99.7% pure C_2H_2 and 99.6% pure C_2H_4 purchased from Takachiho and 99.999% pure Ar from Nippon Sanso. All gases were used without further purification. The test gas was prepared in a 20 l glass bulb manometrically and used after more than 48 h mixing time. The test gas compositions are shown in Table 1.

TABLE 1. MEASURED A AND MODELED $[C_4H_2]$ AND $[C_6H_2]$ AT 2000 K IN EACH TEST GAS MIXTURE (cm and mol units)

No.	Gas composition in Ar	A	$[C_4H_2]/10^{-9}$	$[C_6H_2]/10^{-10}$
1	3.2% C_2H_2	1.11	15	11
2	2.0% C_2H_2/2.3% H_2	0.26	4.3	1.1
3	4.0% C_2H_4	0.94	10	2.0

The test section of the shock tube was evacuated to less than 10^{-4} Torr before each run. Neither emission from C_2H_2 or C_2H_4 in Ar mixtures nor absorption by Ar was observed under the present experimental conditions. (1 Torr=133.322 Pa)

Computer modeling was done using the program mentioned previously.[10] The flow model used for reflected shock waves was modified and a constant density calculation was adopted.[11] Thermochemical properties of the species which appear in the reaction mechanism were taken from the JANAF thermochemical table [12] or other available sources.[9,13,14]

Results and Discussion

A sample oscillogram of the UV absorption (216 nm, 3.2% C_2H_2 in Ar, and $P_2=0.35$ atm) is shown in Fig. 1. We evaluated absorptivities of C_2H_2 and C_2H_4 from the absorption at the shock front for two wavelengths, 216 and 230 nm, by using the following definition:

$$a = \ln(I_0/I)/[C]_0/d,$$

where I_0=incident light intensity, I=transmitted intensity at the shock front, $[C]_0=C_2H_2$ or C_2H_4 concentration at the shock front, and d=optical path length (7.2 cm). The obtained a values of C_2H_2 and C_2H_4 are shown in Figs. 2a and 2b.

Acetylene shows an absorption due to the electronic transition X→A in the wavelength region 210—237

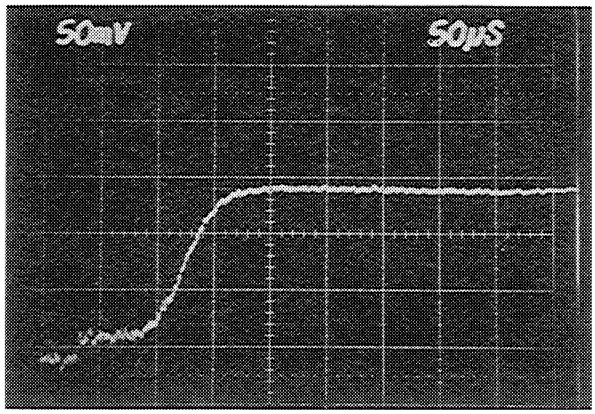

Fig. 1. A representative profile of transmitted D_2-lamp intensity for 3.2% C_2H_2 in Ar mixture, T_2=2084 K, and P_2=0.35 atm.

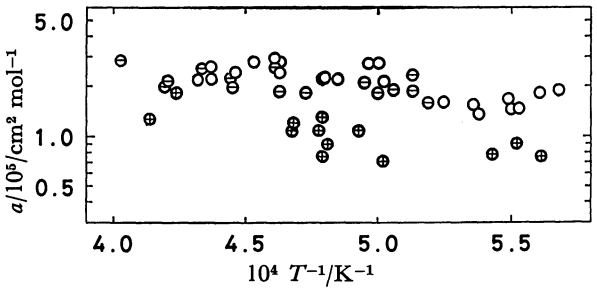

Fig. 2a. Temperature dependence of C_2H_2 absorptivity at 216 and 230 nm with D_2-lamp. The symbols are as follows.
○: for 3.2/96.8=C_2H_2/Ar at 216 nm, ⊖: for 2.0/2.2/95.8=C_2H_2/H_2/Ar at 216 nm, ⊕: for 3.2/96.8=C_2H_2/Ar at 230 nm.

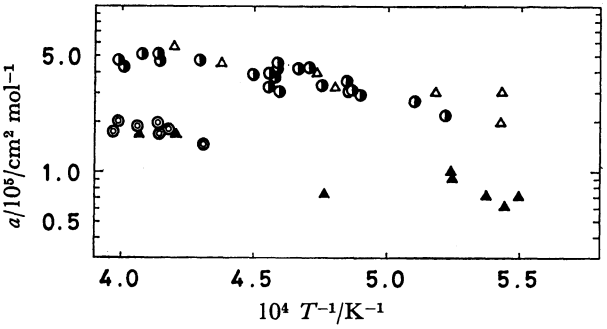

Fig. 2b. Temperature dependence of C_2H_4 absorptivity at 216 and 230 nm. The symbols are as follows.
◑: for 4.0% C_2H_4 in Ar with D_2-lamp at 216 nm,
◎: for 4.0% C_2H_4 in Ar with D_2-lamp at 230 nm,
△: for 4.5% C_2H_4 in Ar with Xe-lamp at 216 nm,
▲: for 4.5% C_2H_4 in Ar with Xe-lamp at 230 nm.
Data taken with Xe-lamp were corrected for higher-order wavelengths.

nm.[15] In comparison with C_2H_2, C_2H_4 has greater absorptivity in this region, though no absorption which can be attributed to an electronic transition is reported for C_2H_4.[15] Figures 2a and 2b show that the absorptivities of C_2H_2 and C_2H_4 at 216 nm are larger than those at 230 nm in the temperature range measured. This may imply that the absorption of C_2H_4 at 216 nm is attributed to an extended transition of X→A. Since the wavelength 230 nm is too far from the wavelength region of the X→A transition, the absorption at 230 nm may not be the extended transition. No clear explanations of the C_2H_4 absorption at 230 nm at these high temperatures can be given only on the basis of the present experimental results.

The a values of C_2H_2 and C_2H_4 increase slightly with increasing temperature, in contrast with the reported a values of CH_3 which have the opposite behavior.[16,17] Similar observations are reported recently for 3.39 μm He–Ne laser absorption of small hydrocarbons, *i.e.*, the infrared a values of C_2H_2 and C_2H_4 increase with increasing temperature, while those of the alkanes decrease with increasing temperature.[18,19]

The absorption measurement at 216 nm was employed to study ethane decomposition and CH_3 recombination in shock waves.[16,17] The results shown above imply that the absorption at 216 nm is not only due to CH_3 but also to C_2H_2 and C_2H_4. For alkane pyrolysis measured at high temperatures, CH_3 is usually formed at an early stage of the reaction and C_2H_2 and C_2H_4 gradually accumulate afterwards. The absorption at 216 nm at the early stage of alkane pyrolysis represents the features of CH_3 alone; the later absorption begins to show aggregate features of CH_3, C_2H_2, and C_2H_4. Our trial runs for the C_2H_6 pyrolysis measured by 230 nm absorption, on the other hand, showed neglibible absorptivity for CH_3 at the 1st stage of the pyrolysis. This result and the above may explain why we selected 216 and 230 nm absorptions to study the C_2H_2 and C_2H_4 pyrolysis. The computer program, which incorporates these absorptivities for C_2H_2 and C_2H_4 at 216 and 230 nm and the absorptivity for CH_3 at 216 nm, may solve the alkane pyrolysis measured at the two wavelengths by a procedure similar to that adopted in the C_2H_6 and C_3H_8 pyrolysis studies monitored by a 3.39 μm He–Ne laser.[14,20]

The oscillogram of Fig. 1 shows that the absorption increases almost linearly after the absorption at the shock front and finally reaches a high plateau value. The plateau absorption A was defined by $A=\ln(I_0/I_f)$, where I_f is the transmitted light intensity at the plateau and I_0 the incident light intensity. In Fig. 3, the relative A value or the value of A divided by the shock front concentration of $[C_2H_2]_0$ or $[C_2H_4]_0$ are shown *vs.* $10^4/T$.

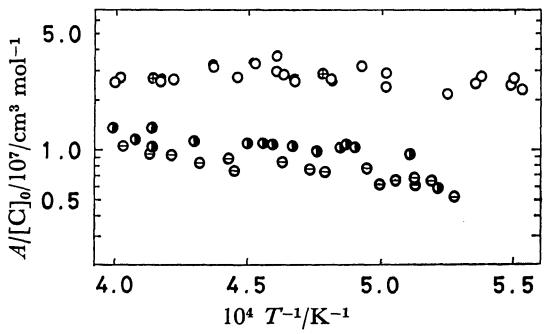

Fig. 3. Temperature dependence of relative steady absorption at 216 and 230 nm. The symbols are as in Figs. 2a and 2b.

In this case, the relative values are free from the choice between the two wavelengths, 216 and 230 nm, but the values show distinct mixture dependence, splitting into two groups as shown in Fig. 3. Searches for the chemical species which are responsible for the plateau absorption were made by the computer modeling, adopting the reaction mechanism shown in Table 2.

TABLE 2. REACTION MECHANISM AND RATE CONSTANTS $k=A\exp(-E/RT)$ (mol, cm, s, and kcal units)

Reaction	log A	E	Ref. No.
1) $C_2H_4+M=C_2H_2+H_2+M$	17.4	79.3	7
2) $C_2H_4+M=C_2H_3+H+M$	17.6	98.2	7
3) $C_2H_4+C_2H_4=C_2H_3+C_2H_5$	14.8	64.0	24
4) $C_2H_4+H=C_2H_3+H_2$	15.7	22.9	7
5) $C_2H_3+C_2H_4=C_4H_6+H$	12.0	7.3	25
6) $C_2H_3+H=C_2H_2+H_2$	13.0	0.	14
7) $C_2H_5+M=C_2H_4+H+M$	15.3	30.1	14
8) $C_2H_2+M=C_2H+H+M$	16.6	106.5	1
9) $C_2H_2+C_2H_2=C_4H_3+H$	12.3	45.0	6
10) $C_2H_3+M=C_2H_2+H+M$	14.9	31.0	25
11) $C_2H_2+C_2H_3=C_4H_4+H$	13.2	25.0	6
12) $C_4H_4+C_2H=C_4H_3+C_2H_2$	13.6	0.	6
13) $C_2H+H_2=C_2H_2+H$	12.4	0.	This work
14) $C_2H_2+C_2H=C_4H_2+H$	13.6	0.	2
15) $C_4H_3+M=C_4H_2+H+M$	16.0	60.0	2
16) $C_4H_2+M=C_4H+H+M$	17.5	80.0	2
17) $C_6H_2+M=C_6H+H+M$	16.7	80.0	2
18) $C_8H_2+M=C_8H+H+M$	16.7	80.0	2
19) $H_2+M=2H+M$	12.4	92.6	26
	$+0.5\log T$		
20) $C_4H_3+H+M=C_4H_4+M$	15.0	0.	2
21) $C_2H_2+C_4H=C_6H_2+H$	13.6	0.	2
22) $C_4H_2+C_2H=C_6H_2+H$	13.6	0.	2
23) $C_2H_2+C_6H=C_8H_2+H$	12.0	0.	2
24) $C_6H_2+C_2H=C_8H_2+H$	12.0	0.	2
25) $C_4H_2+C_4H=C_8H_2+H$	12.0	0.	2

Acetylene radical and polyacetylene radicals can not be the absorbers; if they were, they must have large, temperature-dependent absorptivities. For example, the steady concentration of C_2H at 2500 K is about 20 times larger than that at 2000 K in 3.2% C_2H_2 in Ar mixtures. This means that the absorptivity of C_2H decreases by a similar factor between the two temperatures, because the A values are almost constant over the temperature range measured. We are unaware of any species having such large, temperature-dependent absorptivity.

Table 1 shows the A values, obtained by a least squares fitting for the $A/[C]_0$ and $10^4/T$ relation shown in Fig. 3, and the steady $[C_4H_2]$ and $[C_6H_2]$, obtained by the computer modeling, at 2000 K in different three mixtures. The ratios of the A values, A_m/A_n, are not in accord with the $[C']_m/[C']_n$ values, where subscripts m and n denote the mixture number shown in Table 1 and C' is C_4H_2 or C_6H_2. Although these modeled $[C_4H_2]$ and $[C_6H_2]$ are subject to the values of heat of formation adopted, no clear-cut explanation with appropriate thermochemical data could be given.

There is an electronic transition designated as X→B over the wavelength range 200 to 265 nm for C_4H_2.[15] The reported C_4H_2 profiles in the C_2H_2 pyrolysis measured by TOF mass spectroscopy[4] are similar to the absorption profile of Fig. 1. These results strongly support the conjecture that the steady absorption is mainly due to C_4H_2. The absorptivity of C_4H_2 was evaluated as: $a(\mathrm{cm^2\ mol^{-1}})=(1.1\pm0.3)\times10^7$ at 2000 K and $(1.4\pm0.2)\times10^7$ at 2500 K.

The plateau absorption shown in Fig. 1 indicates that the overall reaction of the C_2H_2 and C_2H_4 pyrolysis reaches an equilibrium under the present experimental conditions; this was confirmed also by the computer modeling. The primary reactions of the C_2H_2 pyrolysis in these temperature ranges are:[6]

$$H + C_2H_2 = H_2 + C_2H \qquad (-13)$$

$$C_2H + C_2H_2 = C_4H_2 + H. \qquad (14)$$

Ethynyl, C_2H, and H play roles as chain carriers in the reactions. An equilibrium between these species leads to an equilibrium for $[C_4H_2]$:

$$[C_4H_2] = K_{-13}K_{14}[C_2H_2]^2/[H_2],$$

where K_{-13} and K_{14} are the equilibrium constants of the reactions, (−13) and (14). The above equation is in accordance with the result shown in Fig. 3 that the presence of H_2 inhibits the formation of C_4H_2, which is one of the precursors to soot.[8] Relative A values in the C_2H_4/Ar mixture are smaller than those in the C_2H_2/Ar mixture. This result also can be explained in the same way. Ethylene decomposes by a molecular reaction fairly rapidly in this temperature range[7] and forms C_2H_2 and H_2 in equal amounts. Therefore, in the C_2H_4/Ar mixture, C_4H_2 is produced by the pyrolysis of C_2H_2 so formed in the presence of H_2. The fact that the measured relative A values in the C_2H_4/Ar and C_2H_2/H_2/Ar mixtures are similar to each other may support the above explanation.

Figure 1 provides us with time parameters whose value can be used as a measure to estimate the overall rate of the C_2H_2 and C_2H_4 pyrolysis. In the conventional manner, the induction time can be defined as: the time between the shock arrival and the foot of the linear absorption rise. If the absorptivity of C_4H_2 is exactly known, the threshold value of $[C_4H_2]$ at the foot can be estimated and compared with the modeled $[C_4H_2]$. But there are still uncertainties in the C_4H_2 absorptivity obtained above. Instead, we defined a parameter, t_m: time between the shock arrival and the crossing point where the linear absorption rise and the steady absorption are extrapolated to each other. The parameter, t_m, so defined is independent of the C_4H_2 absorptivity. The modeled t_m was evaluated from the C_4H_2 profile. First of all, we compared the measured t_m with the modeled one using the mechanism and the rate constants in Table 2 except for the k_{13} value in the C_2H_2/Ar mixture. As for the k_{13} value, $10^{13.54}$ in Ref. 6 was used. Figure 4 shows the relation between $t_m[C_2H_2]_0$ or $t_m[C_2H_4]_0$ and $10^4/T$ for the measured and modeled results. As is shown by the broken line, the modeled t_m was found to be smaller than that measured by a similar factor over the temperature range measured. To confirm the correctness of the interpretations for the

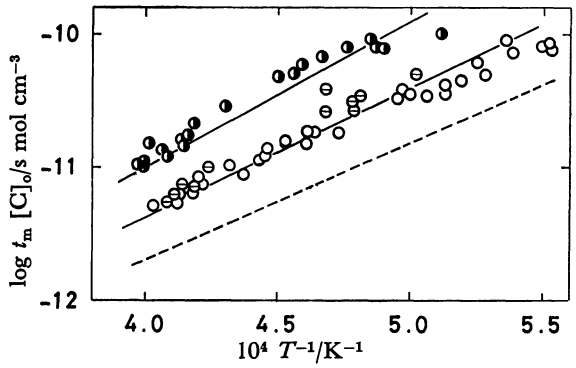

Fig. 4. $t_m[C_2H_2]_o$ or $t_m[C_2H_4]_o$ *vs.* $10^4/T$. The symbols are the same as in Figs. 2a and 2b. The solid lines show modeled value using Table 2 mechanism and rate constants. The upper one is for C_2H_4/Ar mixture and the lower one is for both of C_2H_2/Ar and C_2H_2/H_2/Ar mixtures. The broken line shows modeled value for 3.2% C_2H_2 in Ar mixture using Table 2 mechanism and rate constants except for the k_{13} value: $k_{13}=10^{13.53}$ was used.[6]

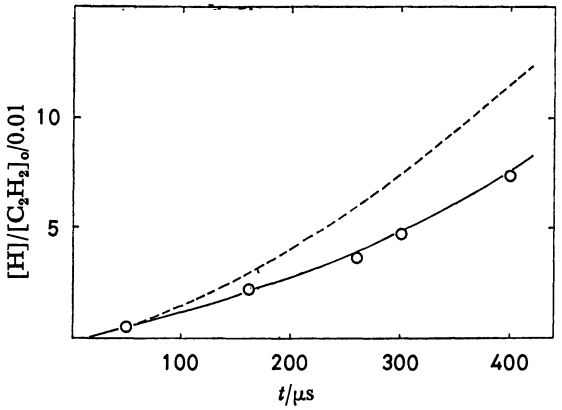

Fig. 5. Comparison measured [H] profile[1] with modeled ones. The circles are data points of measured [H] profile in reflected shock wave for 20 ppm in Ar mixture at $T_5=2450$ K and $[Ar]_5=8.2\times10^{-6}$. The solid and broken lines are modeled values as are in Fig. 4.

present experiment and modeling, another C_2H_2 pyrolysis result was adopted for the modeling.

Gas sampling problems due to boundary layer growth are present in the results obtained by the single pulse shock tube technique.[21] Since TOF mass spectroscopy may also have the same problems, we selected the results obtained by ARAS[1] for the modeling. Figure 5 shows both the measured and the modeled [H] profiles. It is clear that the modeled [H] increasing rate shown by the broken line is larger than the measured one, which is in accordance with the result obtained from Fig. 4, *i.e.*, the modeled overall reaction rate is faster than the measured one.

The first mechanism proposed by Tanzawa and Gardiner,[2] which was derived to explain the high temperature pyrolysis of C_2H_2 in shock waves, could model the results of TOF mass spectroscopy[3,4] and single pulse shock tube[5] fairly well, whereas the new mechanism in Ref. 6 gave rather poor modeling results. The new mechanism in Ref. 6 seems to have an improper

Table 3. Sensitivity spectrum with PS values[a]

Reaction	t_m[b]	$[H]_{100\,\mu s}$[c]	$[H]_{400\,\mu s}$[c]
$C_2H_2+M=C_2H+H+M$	−8/−5[d]	87/97	54/87
$C_2H_2+C_2H_2=C_4H_3+H$	−8/−5	—	—
$C_2H+H_2=C_2H_2+H$	−29/−42	30/47	29/57
$C_2H_2+C_2H=C_4H_2+H$	−3/−18	11/3	25/15
$C_4H_2+M=C_4H+H+M$	−21/−27	—	—

a) PS=log (parameter′/parameter)/log (multiplier)× 100. Details are shown in Ref. 22. b) For 3.2% C_2H_2 in Ar mixture, $P_2=0.37$ atm, and $T_2=2200$ K. c) For 50 ppm C_2H_2 in Ar mixture, $P_5=1.77$ atm, and $T_5=2420$ K. d) The first entry is obtained by multiplying each rate constant by 5; the second entry, by 0.2.

value for some rate constant. To find which reaction is responsible to the disageement shown in Figs. 4 and 5, a sensitivity calculation with PS values[22] was tried for our experiment and for the ARAS measurement.[1]

Table 3 shows the reactions having large PS values and the obtained PS values for the parameters. The reaction which has the largest PS values is different in our experiment and in the ARAS experiment. The effect of secondary reactions on the [H] profile is surpressed in the latter case, in which highly diluted test gas mixtures were used, and the measured and modeled [H] profiles reflect the initiation reaction, $C_2H_2+M=C_2H+H+M$, especially at the early stages of the reaction. The PS values of reaction 14 becomes large as the reaction proceeds, in contrast to those of the initiation reaction, while reaction 13 has an almost constant PS values. The time dependent variations of PS values imply that the chain carrier concentrations such as H and C_2H increase and the chain reactions dominate. These effects of the chain reactions on the parameters adopted are very distinct in our experiment.

Reaction 16, $C_4H_2+M=C_4H+H+M$, has the second largest PS values for t_m in our experiment. Frank and Just[1] measured the k_{16} value in the high pressure limit directly by monitoring the [H] profile produced by the C_4H_2 pyrolysis using the ARAS. Although it is possible to derive the k_{16} value suitable for the modeling of our experiment from the reported k_{16} value by making a reduced fall-off curve,[23] we left the k_{16} value used in this study at the value determined indirectly by Tanzawa and Gardiner,[2] through the computer modeling for the laser schlieren experiment because the experimental conditions selected by them are similar to the present ones except for the temperature range.

Since the C_2H_2 pyrolysis is almost equilibrated at the reaction time when the parameter t_m is measured, it is to be expected that reaction 13 has the largest PS values. So only the k_{13} value was changed so as to fit the modeled t_m to the measured over the temperature range measured. An excellent agreement between the experiment and the modeling for the [H] profiles, as well as for the t_m values, was obtained by adopting the following k_{13} value:

$$k_{13}=10^{12.4}(\mathrm{cm^3\,mol^{-1}\,s^{-1}}).$$

This is shown in Figs. 4 and 5. In our computer

program,[10] reverse rate constant of a given elementary reaction is calculated using an equilibrium constant; an assembly of first order differential equations of both forward and reverse reactions is numerically integrated. Then, when either k_{13} or k_{-13}, where $K_{-13}=k_{-13}/k_{13}$, is incorporated into the reaction mechanism with reasonable thermochemical data, the same modeling results can be obtained. Tanzawa and Gardiner[2] proposed a non-Arrhenius temperature-dependent k_{-13} value in the first mechanism. The k_{13} value so evaluated from the k_{-13} value was found to have exactly the same value at 2200 K as the present k_{13} value. Then, it is not surprising that the k_{13} value obtained in this study is about 10 times smaller than that in Ref. 6.

We note that the modeling result of the C_2H_2 and C_2H_4 pyrolysis is affected by the ΔH°_{f0} value adopted for acetylene and polyacetylene radicals. Two recent papers about the C_2H_2 pyrolysis study[1,2] demonstrated the correctness of the new ΔH°_{f0} for C_2H.[9] As has been shown already, this new value of ΔH°_{f0} for C_2H will be a help to improve the ΔH°_{f0} values for polyacetylene radicals using the additivity rule.[27] The ΔH°_{f0} value for C_4H so derived is 180 kcal†/mol,[1] which is 26 kcal/mol larger than the old value.[13] If the old value for C_4H is adopted, unusual profiles of C_4H_2 and C_4H can be obtained, *e.g.*, steady $[C_4H]$ is larger than steady $[C_4H_2]$.

We have little to say about the C_2H_4 pyrolysis during the early reaction period on the basis of the present experimental results. The computer modeling for the C_2H_4/Ar mixture showed that almost all of C_2H_4 is pyrolyzed to C_2H_2 and H_2 already at the reaction time when the linear absorption starts.

† 1 kcal=4.184 kJ.

References

1) P. Frank and Th. Just, *Ber. Bunsenges. Phys. Chem.*, **81**, 1119 (1977).

2) T. Tanzawa and W. C. Gardiner, Jr., "17th Int. Symp. Combust.," The Combustion Institute, Pittsburgh (1979), p. 563.

3) J. N. Bradley and G. B. Kistiakowsky, *J. Chem. Phys.*, **35**, 264 (1961).

4) I. G. Gay, G. B. Kistiakowsky, J. V. Michael, and H. Niki, *J. Chem. Phys.*, **43**, 1720 (1965).

5) G. B. Skinner and E. M. Sokoloski, *J. Phys. Chem.*, **64**, 1952 (1960).

6) T. Tanzawa and W. C. Gardiner, Jr., *J. Phys. Chem.*, **84**, 236 (1980).

7) Th. Just, P. Roth, and R. Damm, "16th Int. Symp. Combust.," The Combustion Institute, Pittsburgh (1977), p. 961.

8) R. B. Cundall, D. E. Fussey, A. J. Harrison, and D. Lampard, "Proc. 11th Shock Tube Symp.," Univ. Washington Press, Seattle (1977), p. 375.

9) H. Okabe and V. H. Dibeler, *J. Chem. Phys.*, **59**, 2430 (1973).

10) T. Koike and K. Morinaga, *Bull. Chem. Soc. Jpn.*, **49**, 1457 (1976).

11) W. C. Gardiner, Jr., B. F. Walker, and C. B. Wakefield, "Shock Waves in Chemistry," ed by A. Lifshitz, Dekker, New York (1980), Chap. 1.

12) D. R. Stull and H. Prophet, "JANAF Thermochemical Tables," 2nd ed, NSRDS-NBS 37 (1971).

13) R. S. Duff and S. H. Bauer, *J. Chem. Phys.*, **36**, 1754 (1962).

14) D. B. Olson, T. Tanzawa, and W. C. Gardiner, Jr., *Int. J. Chem. Kinet.*, **11**, 23 (1979).

15) G. Hertzberg, "Molecular Spectra and Molecular Structure," D. Van Nostrand, N. J. (1966), Vol. 3.

16) K. Glänzer, M. Quack, and J. Troe, "16th Int, Symp, Combust.," The Combustion Institute, Pittsburgh (1977). p. 949.

17) T. Tsuboi, *Jpn. J. Appl. Phys.*, **17**, 709 (1978).

18) D. B. Olson, W. G. Mallard, and W. C. Gardiner, Jr., *Appl. Spectrosc.*, **32**, 48 (1978).

19) T. Koike and W. C. Gardiner, Jr., *Appl. Spectrosc.*, **34**, 81 (1980).

20) T. Koike and W. C. Gardiner, Jr., *J. Phys. Chem.*, in press.

21) G. B. Skinner, *Int. J. Chem. Kinet.*, **9**, 863 (1977).

22) W. C. Gardiner, Jr., *J. Phys. Chem.*, **81**, 2367 (1977).

23) J. Troe, *J. Phys. Chem.*, **83**, 114 (1979).

24) M. L. Boyd, T. M. Mu, and M. H. Back, *Can. J. Chem.*, **46**, 2415 (1968).

25) S. W. Benson and G. R. Haugen, *J. Phys. Chem.*, **71**, 1735 (1967).

26) A. L. Myerson and W. S. Watt, *J. Chem. Phys.*, **49**, 425 (1968).

27) S. W. Benson, "Thermochemical Kinetics," 2nd ed, Wiley, New York (1976).